

Structural, Electronic and Elastic Properties of GaN-Ti Bulk and Nanotubes

NEW MATERIAL DEVELOPMENT WITH BIOVIA (CUTM 3110)

by

Kirti Vardhan Singh (Roll No. 210301120137)

Under the Guidance of
Dr. Padmaja Patnaik



**Centurion
UNIVERSITY**

**SCHOOL OF ENGINEERING AND TECHNOLOGY
BHUBANESWAR CAMPUS
CENTURION UNIVERSITY OF TECHNOLOGY AND
MANAGEMENT
ODISHA**

July 2024 / November 2024

DEPARTMENT OF COMPUTER SCIENCE AND ENGINEERING

SCHOOL OF ENGINEERING AND TECHNOLOGY
BHUBANESWAR CAMPUS

BONAFIDE CERTIFICATE

Certified that this project report "Structural, Electronic and Elastic Properties of GaN-Ti Bulk and Nanotubes" is the bonafide work of "Kirti Vardhan Singh" who carried out the project work under my supervision. This is to certify that this project has not been carried out earlier in this institute and the university to the best of my knowledge.

(Dr. Padmaja Patnaik)
Professor, Dept. of Physics, SoAS

Certified that the project mentioned above has been duly carried out as per the college's norms and the university's statutes.

Dr. Sujata Chakravarty
Dean, SoET

Mr. Rajkumar Mohanta
HoD, Dept. of CSE, SoET

DECLARATION

We hereby declare that the project entitled “Structural, Electronic and Elastic Properties of GaN-Ti Bulk and Nanotubes” submitted for the “NEW MATERIAL DEVELOPMENT WITH BIOVIA ” of 7th semester B. Tech in Computer Science and Engineering our original work and the project has not formed the basis for the award of any Degree / Diploma or any other similar titles in any other University / Institute.

Kirti Vardhan Singh 210301120137

Place:Jatni

Date:

ACKNOWLEDGEMENTS

We wish to express our profound and sincere gratitude to Prof. Dr. Padmaja Patnaik, Department of Electronics & Communication Engineering, SoET, Bhubaneswar Campus, who guided me into the intricacies of this project nonchalantly with matchless magnanimity.

We thank Prof. Raj Kumar Mohanta, Head of the Dept. of Department of Computer Science and Engineering, SoET, Bhubaneswar Campus for extending their support during this investigation.

We would be failing in my duty if we didn't acknowledge the cooperation rendered during various stages of image interpretation by Dr. Padmaja Patnaik.

We are grateful to Prof. Sujata Chakrabarty, Dean, School of Engineering and Technology, Bhubaneswar Campus. who evinced keen interest and invaluable support in the progress and successful completion of our project work.

We are indebted to our faculty members for their constant encouragement, cooperation, and help. Words of gratitude are not enough to describe the accommodation and fortitude that they have shown throughout our endeavor.

Kirti Vardhan Singh 210301120137

Place: Jatni

Date:

Abstract

This project investigates the structural, electronic, and elastic properties of titanium (Ti)-doped gallium nitride (GaN) in bulk and nanotube forms using advanced computational tools. Density functional theory (DFT) simulations with CASTEP were applied to analyze the Brillouin zone, bandgap, and band structure, revealing that Ti doping reduces the band gap of GaN, thus enhancing its electronic conductivity. Calculations of the Density of States (DOS) and Partial Density of States (PDOS) further demonstrated how Ti-induced impurity levels affect the electronic structure. Using the Forcite module, molecular dynamics simulations were performed to assess mechanical properties, indicating that Ti-doped GaN nanotubes exhibit improved elasticity and mechanical strength compared to pure GaN, with distinct advantages in flexibility and thermal stability. These findings highlight the potential of GaN-Ti materials for applications in nanoelectronics, optoelectronics, and high-stress environments, underscoring the role of doping in tuning material properties for specific functional needs.

Contents

Bonafide Certificate	i
Declaration	ii
Acknowledgements	iii
Abstract	iii
1 Introduction	6
2 Computational Method	6
3 Results & Discussion	8
3.1 Calculation and Analysis using CASTEP tool	8
3.1.1 Brillouin Zone	12
3.1.2 Bandgap and Band structure	14
3.1.3 Effect of Titanium (Ti) Doping on the Band Structure and Band Gap of GaN	17
3.1.4 Density of States and Partial Density of States	18
3.2 Calculation and analysis using Forceit tool	22
3.3 Mechanical properties	24
4 Conclusion	30
5 References	31

List of Figures

1	GaN-Ti (8,0) SWNT k-points	10
2	GaN-Ti (9,0) SWNT k-points	10
3	GaN-Ti (10,0) SWNT k-points	10
4	GaN-Ti (8,0) SWNT cut-off energy	10
5	GaN-Ti (8,0) 32 Atoms	11
6	GaN-Ti (9,0) 36 Atoms	11
7	GaN-Ti (10,0) 40 Atoms	12
8	GaN-Ti crystal 32 Atoms	12
9	The first and second Brillouin zones of a two-dimensional square lattice	12
10	Structure of Brillouin Zone: (a) GaN-Ti (8,0) with 32 atoms, (b) GaN-Ti (9,0) with 36 atoms, (c) GaN-Ti (10,0) with 40 atoms, and (d) GaN-Ti crystal with 32 atoms.	13
11	A band gap diagram showing the different sizes of band gaps for conductors, semiconductors, and insulators	14
12	Band Structure of GaN-Ti Nanotube(8,0)	15
13	Band Structure of GaN-Ti Nanotube(9,0)	15
14	Band Structure of GaN-Ti Nanotube(10,0)	15
15	Band Structure of GaN-Ti Bulk crystal	16
16	Density of states and partial density of states plot of one Titanium atom doped at $3 \times 3 \times 6$ k-points (a) GaN (8,0) (b) GaN (9,0) (c) GaN (10,0)	19
17	Density of states and partial density of states plot of one Titanium atom doped at $3 \times 3 \times 6$ k-points (a) GaN (8,0) (b) GaN (9,0) (c) GaN (10,0)	20
18	one Titanium atom doped with GaN (a) GaN-Ti (8,0), (b) GaN-Ti (9,0), (c) GaN-Ti (10,0), and (d) GaN-Ti crystal.	21
19	Brillouin Zone Structure obtained through Geometry optimization GaN with Ti doped: (a) GaN-Ti (8,0), (b) GaN-Ti (9,0), (c) GaN-Ti (10,0), and (d) GaN-Ti crystal.	23
20	Mechanical properties of Geometry optimized GaN-Ti bulk crystal: (a) Shear modulus, (b) Poissons ratio, (c) Youngs modulus, and (d) Linear compressibility.	25
21	Mechanical properties of Geometry optimized GaN-Ti SWNT (8,0): (a) Linear compressibility, (b) Shear modulus, (c) Poissons ratio, and (d) Youngs modulus.	26
22	Mechanical properties of Geometry optimized GaN-Ti SWNT (9,0): (a) Linear compressibility, (b) Shear modulus, (c) Poissons ratio, and (d) Youngs modulus.	27
23	Mechanical properties of Geometry optimized GaN-Ti SWNT (10,0): (a) Linear compressibility, (b) Shear modulus, (c) Poissons ratio, and (d) Youngs modulus.	28

List of Tables

1	Lattice parameters and cell angles for GaN-Ti nanotubes in Forcite calculation	7
2	Lattice parameters and cell angles for GaN-Ti nanotubes in CASTEP calculation	7
3	Electronic parameters from the GaN-Ti CASTEP calculation	7
4	GaN Nanotube Doping Information	20
5	Mechanical properties Bulk and SWNT structures	29

1 Introduction

After the discovery of nanotubes, particularly carbon nanotubes, researchers have been actively seeking other stable and efficient nanotubes through various experimental and computational methods. Materials such as gallium nitride (GaN) and titanium (Ti) have attracted significant attention due to their unique semiconductor properties, which remain consistent regardless of tube chirality, unlike carbon nanotubes whose metallic or semiconducting behavior depends on the chirality and diameter. GaN-Ti nanotubes are polar in nature due to the differences in electronegativity between the Ga-N and Ti atoms, whereas carbon nanotubes are non-polar. Additionally, the bond length in GaN-Ti nanotubes is larger than that of carbon-carbon bonds, which suggests potential applications in storage and energy-related fields. GaN-Ti composites combine the exceptional thermal and mechanical properties of GaN with the high strength and corrosion resistance of Ti.

In this study, we focus on the optimization and stabilization of GaN-Ti bulk structures and nanotubes with varying chiralities, specifically (8,0), (8,7), and (8,8) configurations. Using first-principles calculations, phonon dispersion curves, and thermodynamic properties like free energy and heat capacity are analyzed. Doping and functionalization are explored to understand how these properties can be tuned for potential applications in nanoelectronics and energy storage devices.

2 Computational Method

Density functional theory (DFT) using the Kohn-Sham equation was employed via BIOVIA Material Studio to calculate the phonon dispersion and thermodynamic properties for GaN-Ti bulk material and GaN-Ti single-walled nanotubes (SWNTs). Calculations were carried out using the Generalized Gradient Approximation (GGA) with the Perdew-Burke-Ernzerhof (PBE) functional. Phonon dispersion relations were computed for bulk GaN-Ti and (8,0), (9,0), and (10,0) zigzag nanotube configurations.

The atomic masses used were 69.723 AMU for Ga, 14.0067 AMU for N, and 47.867 AMU for Ti. For pseudopotentials, files `Ga_00.usp`, `N_00.usp`, and `Ti_00.usp` were utilized. The charge spilling parameter was set to 1.05%.

Phonon dispersion calculations were performed using the CASTEP module in BIOVIA, and different k-points were chosen to optimize the phonon frequencies and ensure convergence. A Monkhorst-Pack grid of $4 \times 4 \times 6$ was used for bulk, while a $1 \times 1 \times 10$ grid was used for the nanotube configurations. Phonon modes were calculated at the Gamma point ($1 \times 1 \times 1$) and along various high-symmetry directions.

Thermodynamic properties, including free energy, entropy, and heat capacity, were calculated from the phonon density of states (PDOS). Data for

both bulk GaN-Ti and nanotubes were compared to analyze size-dependent variations in thermal behavior. Additionally, total and partial density of states were computed for thermodynamic analysis of the Ti-doped GaN structures.

All calculations for phonon properties and thermodynamic parameters were plotted using Origin software, and the results were validated through convergence tests of the Monkhorst-Pack grids and energy cut-off points.

Table 1: Lattice parameters and cell angles for GaN-Ti nanotubes in Force calculation

GaN-Ti Nanotube	Nanotube cell volume In A^3	Lattice Parameters			Cell angles		
		a	b	c	α	β	γ
GaN-Ti (10,0)	864.921	12.5156	15.1948	5.42068	88.58	94.23	122.70
GaN-Ti (9,0)	722.169	11.1169	14.5399	5.38125	77.97	104.15	120.61
GaN-Ti (8,0)	611.432	12.0386	10.0953	5.35976	92.17	101.87	105.45

Table 2: Lattice parameters and cell angles for GaN-Ti nanotubes in CASTEP calculation

GaN-Ti Nanotube	Nanotube cell volume In A^3	Lattice Parameters			Cell angles		
		a	b	c	α	β	γ
GaN-Ti (10,0)	460.789	11.1758	11.1758	4.260	90	90	120
GaN-Ti (9,0)	398.492	10.3929	10.3929	4.260	90	90	120
GaN-Ti (8,0)	340.718	9.610	9.610	4.260	90	90	120

Table 3: Electronic parameters from the GaN-Ti CASTEP calculation

	GaN-Ti (10,0)	GaN-Ti (9,0)	GaN-Ti (8,0)
Number of Doping atom	one Ti atom	one Ti atom	one Ti atom
Number of electrons	359	323	287
Number of bands	180	162	144
Eigen-energy convergence tolerance (10^{-6} eV)	0.1111	0.1111	0.1111

3 Results & Discussion

3.1 Calculation and Analysis using CASTEP tool

The phonon and thermodynamic properties of GaN-Ti bulk and nanotubes originate from the structural foundation, analogous to carbon nanotubes (CNT). In GaN-Ti nanotubes, the chiral vector can be expressed as:

$$h = \mathbf{a}_1 + \mathbf{a}_2 = (n, m)$$

where n and m are integers defining the nanotube's structure. \mathbf{a}_1 and \mathbf{a}_2 represent the real-space unit vectors of the lattice. Chiral GaN-Ti nanotubes follow the condition:

$$0 < |m| < n$$

Special cases include armchair nanotubes, defined by $h = (n, n)$, and zigzag nanotubes, defined by $h = (n, 0)$. These structural configurations influence the phonon dispersion and thermodynamic stability.

The phonon modes, essential for understanding thermal conductivity and stability, are sensitive to both the chirality and diameter of the nanotubes. GaN-Ti bulk materials exhibit distinct thermodynamic properties compared to their nanotube counterparts, with the reduced dimensionality of nanotubes significantly impacting specific heat and thermal expansion.

Generally, GaN-Ti nanotubes exhibit diverse phonon and thermodynamic properties based on their structural configuration, such as armchair or zigzag. Armchair GaN-Ti nanotubes are known for their stability and enhanced thermal conductivity. However, unlike carbon nanotubes that exhibit metallic behavior, the thermodynamic characteristics of GaN-Ti nanotubes are significantly influenced by their chirality and diameter.

For GaN-Ti bulk materials, the phonon dispersion and specific heat are impacted by reduced dimensionality when transitioning to nanotube form. These nanotubes display modified thermal expansion behavior, and the phonon modes become more sensitive to structural variations. Furthermore, doping GaN-Ti nanotubes with metal atoms alters their thermal and mechanical properties, potentially leading to improved stability or unique phonon behaviors. This modification can result in shifts in thermodynamic stability and changes in specific heat capacity, essential for high-temperature applications.

The unique thermodynamic properties of GaN-Ti nanotubes, including enhanced heat dissipation and tunable specific heat, arise from their nanoscale structure, making them promising candidates for advanced thermal management systems. The electronic configuration of materials used in this work are as follows: -

$$\begin{aligned}
\mathbf{Ga} &: 1s^2 2s^2 2p^6 3s^2 3p^6 3d^{10} 4s^2 4p^1 \\
\mathbf{N} &: 1s^2 2s^2 2p^3 \\
\mathbf{Ti} &: 1s^2 2s^2 2p^6 3s^2 3p^6 3d^2 4s^2
\end{aligned}$$

Pseudo atomic calculation performed for N at $2s^2 2p^3$ converged in 14 iterations to a total energy of -108.7592 eV. Pseudo atomic calculation for Ga at $3d^{10} 4s^2 4p^1$ converged in 17 iterations to a total energy of -596.7205 eV. Pseudo atomic calculation performed for Ti at $3d^2 4s^2$ converged in 45 iterations to a total energy of -1574.376 eV.

The plane wave basis set cut-off used after minimizing the energy curve for GaN-Ti was set at 350 eV. The maximum number of SCF cycles used for the calculations was 120. The Pulay density-mixing scheme was applied to achieve convergence.

For phonon and thermodynamic properties, the phonon dispersion curves were calculated to assess vibrational stability, and specific heat capacity at constant volume (C_v) was derived from phonon density of states. The calculated isobaric heat capacity (C_p) and thermal expansion coefficients were consistent with first-principles simulations of bulk and nanotube structures.

A graph representing the total energy of a GaN-Ti nanotube structure as a function of the number of k-points employed in this computation (Fig. 1, 2, 3). K-points are a discrete collection of points in reciprocal space used in numerical calculations to depict the continuous Brillouin zone. The total energy value converges on the k-points vs. total energy curve as the number of k-points increases, leading to improved accuracy in the estimated total energy.

This curve helps identify the ideal number of k-points required for calculations with the appropriate level of precision. The graphs of k-points versus total energy in Fig. 1, Fig. 2, and Fig. 3 correspond to different configurations of GaN-Ti nanotubes. The minimal total energy is achieved at $2 \times 2 \times 3$ k-points. Consequently, by fixing the k-points, the minimal cut-off energy is found to be approximately 550 eV, as shown in Fig. 4.

A graph illustrating the total energy of a single-walled nanotube structure as a function of the calculation's cut-off energy (Fig. 4). In electronic structure calculations, the cut-off energy is a critical parameter that establishes an upper bound on the energy of interactions between electrons and ions in a system.

As the cut-off energy increases, the accuracy of the computed total energy improves, leading to convergence on the cut-off energy versus total energy curve. This curve is essential for identifying the optimal cut-off energy necessary to achieve the desired level of calculation accuracy.

Moreover, the choice of cut-off energy affects both the computation time and the precision of the results. While a higher cut-off energy generally results in increased computational costs, it also yields more accurate results.

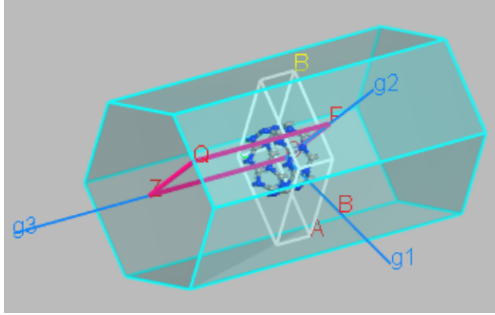


Figure 1: GaN-Ti (8,0) SWNT k-points

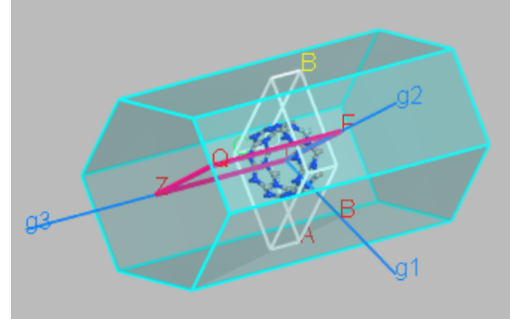


Figure 2: GaN-Ti (9,0) SWNT k-points

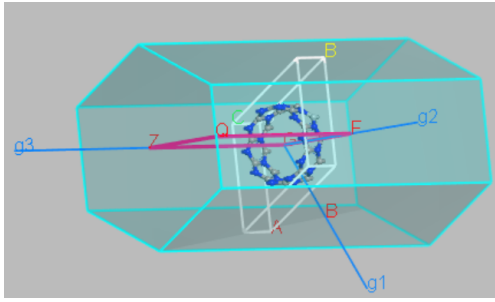


Figure 3: GaN-Ti (10,0) SWNT k-points

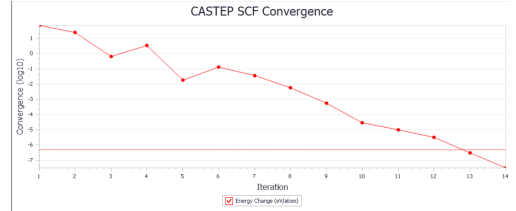


Figure 4: GaN-Ti (8,0) SWNT cut-off energy

Three different single-walled gallium nitride-titanium (GaN-Ti) nanotubes are illustrated by the structures of GaN-Ti (8,0) with 32 atoms, GaN-Ti (9,0) with 36 atoms, and GaN-Ti (10,0) with 40 atoms in fig given. In these structures, gallium atoms are depicted in blue, nitrogen atoms in green, and titanium atoms in grey. The nanotubes' chiral indices, denoted by the numbers in parentheses, determine their geometry. These indices (n, m) represent the number of unit vectors along the circumference of the nanotube, corresponding to the lattice vectors from the hexagonal GaN sheet from which the nanotube is derived. Each nanotube has a cylindrical shape with an arrangement of atoms forming hexagons. As the diameter increases with higher chiral indices, the total number of atoms increases, leading to a rise in the total energy and adding complexity to the electronic structure.

The first Brillouin zones of each of the single-walled nanotubes depicted in Fig. 6 are represented by the Brillouin zones of GaN-Ti (8,0) SWNT, GaN-Ti (9,0) SWNT, and GaN-Ti (10,0) SWNT. The periodic recurrence of a crystal lattice's electronic structure in reciprocal space is referred to as the Brillouin zone, which is a fundamental concept in solid-state physics. In the case of GaN-Ti nanotubes, the periodic boundary conditions of the

nanotube's circumference and the hexagonal arrangement of gallium, nitrogen, and titanium atoms play a significant role in determining the Brillouin zones. The chiral indices of the nanotubes, which dictate the geometry of the nanotubes, also influence the shape and structure of the Brillouin zones.

Due to their various diameters and geometries, GaN-Ti (8,0) SWNT, GaN-Ti (9,0) SWNT, and GaN-Ti (10,0) SWNT exhibit different Brillouin zones. As the nanotube diameter increases, the Brillouin zone expands, leading to a more complex electronic structure. The electronic band structures of these nanotubes, which define the allowed energy levels for electrons, are derived from their respective Brillouin zones. These band structures provide critical information about the electrical properties of the nanotubes, especially their conductivity.

A smaller band gap suggests higher conductivity, making such nanotubes suitable as electrical conductors or components in electronic devices. Conversely, a larger band gap indicates lower conductivity, making the nanotubes more suitable as insulators. The band gap characteristics of GaN-Ti nanotubes are crucial for potential applications, as they can be tailored for specific uses. GaN-Ti nanotubes are attractive for various applications in electronics, energy storage, and sensing, thanks to their unique electronic properties. Their versatility stems from the ability to adjust the band gap and, consequently, the electrical behavior through changes in geometry and composition.

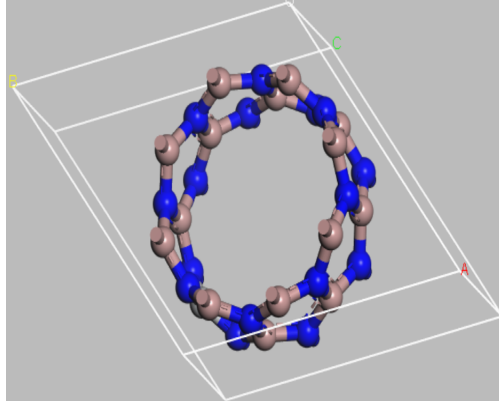


Figure 5: GaN-Ti (8,0) 32 Atoms

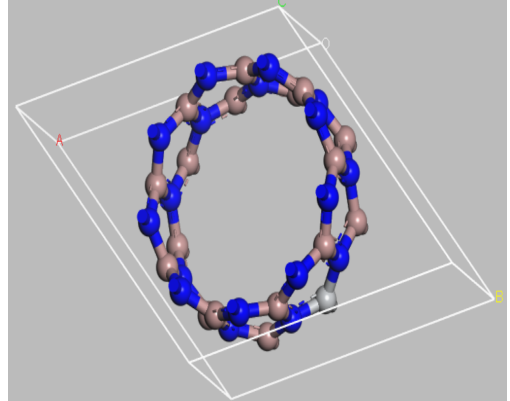


Figure 6: GaN-Ti (9,0) 36 Atoms

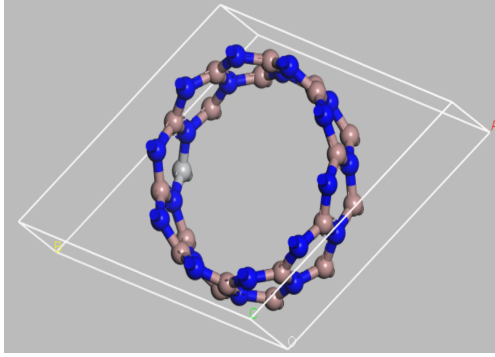


Figure 7: GaN-Ti (10,0) 40 Atoms

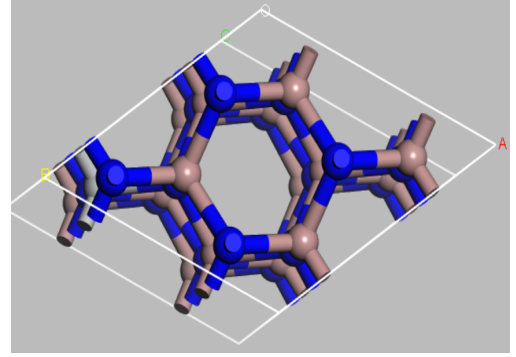


Figure 8: GaN-Ti crystal 32 Atoms

3.1.1 Brillouin Zone

A Brillouin zone is defined as a Wigner-Seitz primitive cell in the reciprocal lattice. The first Brillouin zone is the smallest volume entirely enclosed by planes that are the perpendicular bisectors of the reciprocal lattice vectors drawn from the origin. The concept of the Brillouin zone is particularly important in the consideration of the electronic structure of solids.

There are also second, third, etc., Brillouin zones, corresponding to a sequence of disjoint regions (all with the same volume) at increasing distances from the origin, but these are used more rarely. As a result, the first Brillouin zone is often called simply the Brillouin zone. In general, the n-th Brillouin zone consists of the set of points that can be reached from the origin by crossing $n - 1$ Bragg planes.

The region in k-space (here an imaginary plane whose rectangular coordinates are k_x and k_y) that low-k electrons can occupy without being diffracted is called the first Brillouin Zone, shown in Figure 1. The second Brillouin zone is also shown; it contains electrons with k values from $\frac{\pi}{a}$ to $\frac{2\pi}{a}$ for electrons moving in the $\pm x$ and $\pm y$ directions, with the possible range of k values narrowing as the diagonal directions are approached.

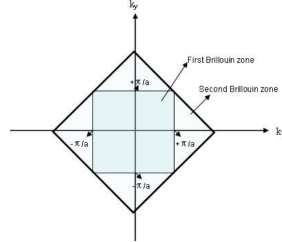


Figure 9: The first and second Brillouin zones of a two-dimensional square lattice

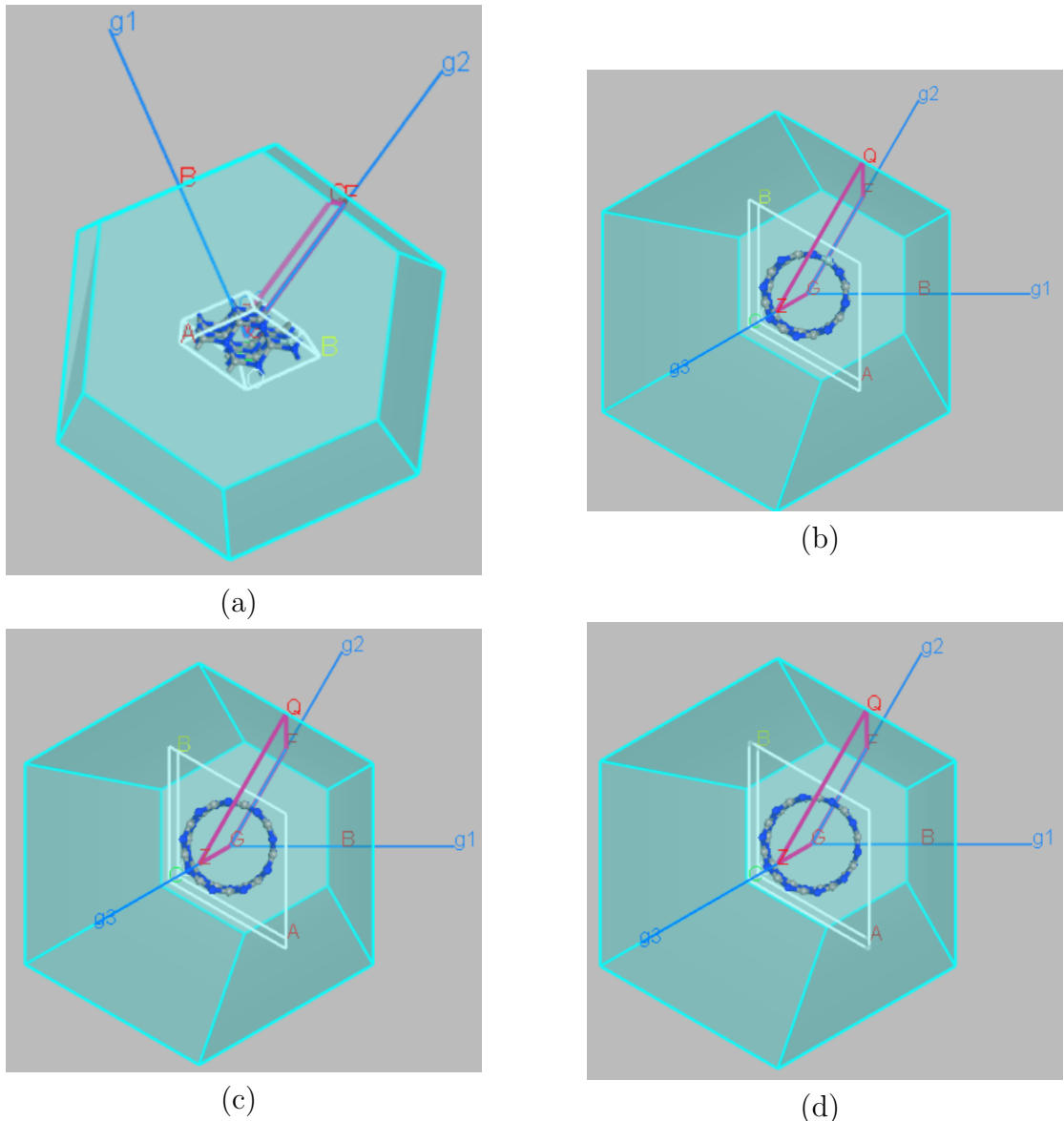


Figure 10: Structure of Brillouin Zone: (a) GaN-Ti (8,0) with 32 atoms, (b) GaN-Ti (9,0) with 36 atoms, (c) GaN-Ti (10,0) with 40 atoms, and (d) GaN-Ti crystal with 32 atoms.

3.1.2 Bandgap and Band structure

A band gap is the distance between the valence band of electrons and the conduction band. Essentially, the band gap represents the minimum energy that is required to excite an electron up to a state in the conduction band where it can participate in conduction. The lower energy level is the valence band, and thus if a gap exists between this level and the higher energy conduction band, energy must be input for electrons to become free. The size and existence of this band gap allows one to visualize the difference between conductors, semiconductors, and insulators. These distances can be seen in diagrams known as band diagrams, shown in Figure 10 below.

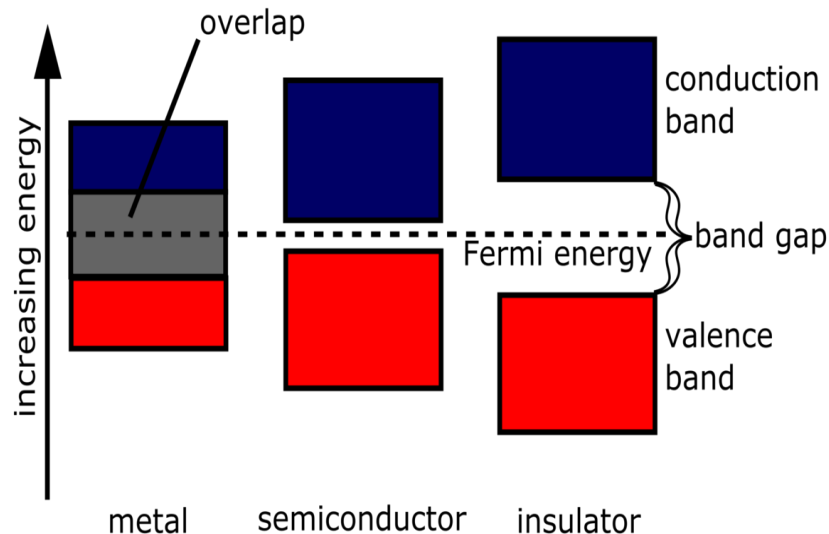


Figure 11: A band gap diagram showing the different sizes of band gaps for conductors, semiconductors, and insulators

Figure 11 above illustrates the difference in size of the band gap for insulators, conductors, and semiconductors. The size of this band gap gives the materials some of their distinct properties. In insulators, the electrons in the valence band are separated by a large band gap from the conduction band. This means that there is a large "forbidden" gap in energies preventing electrons from the valence band from jumping up into the conduction band and participating in conduction. This provides an explanation for why insulators do not conduct electricity well.

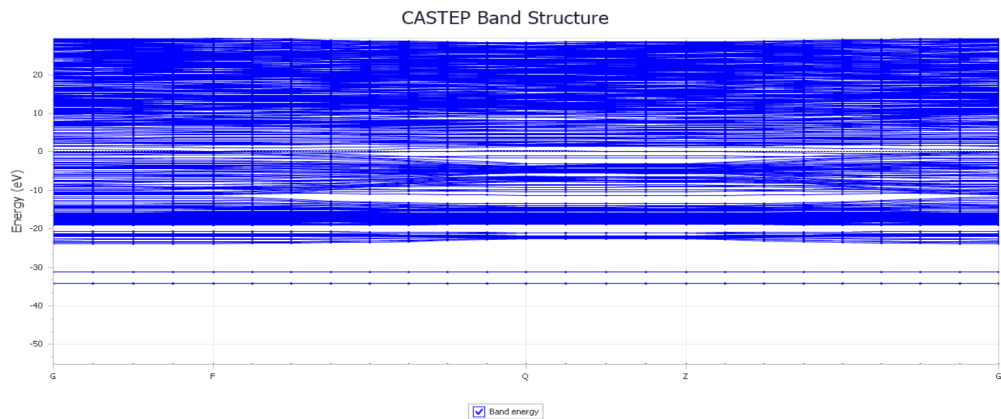


Figure 12: Band Structure of GaN-Ti Nanotube(8,0)

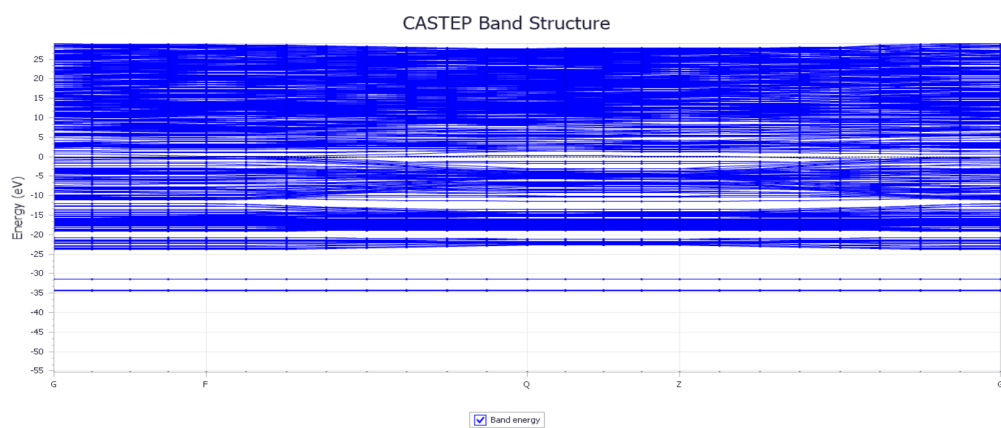


Figure 13: Band Structure of GaN-Ti Nanotube(9,0)

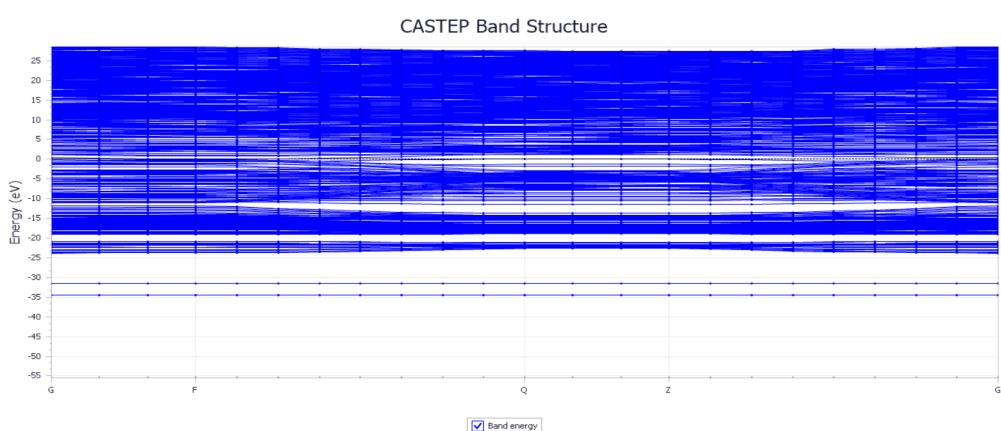


Figure 14: Band Structure of GaN-Ti Nanotube(10,0)

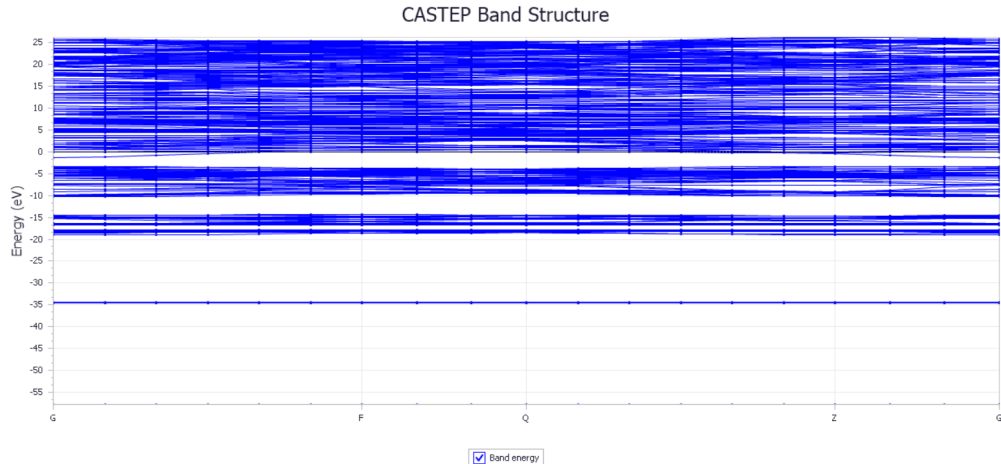


Figure 15: Band Structure of GaN-Ti Bulk crystal

Bandgap Energy Calculation

The bandgap energy of a material is calculated by subtracting the energy of the valence band maximum (VBM) from the energy of the conduction band minimum (CBM). The formula is given by:

$$\text{Bandgap} = \text{Energy of CBM} - \text{Energy of VBM}$$

Bandgap Values:

1. - Bandgap for GaN-Ti Nanotube (8,0) = 1.799 eV
2. - Bandgap for GaN-Ti Nanotube (9,0) = 1.523 eV
3. - Bandgap for GaN-Ti Nanotube (10,0) = 1.437 eV
4. - Bandgap for GaN-Ti Bulk Crystal = 0.43361 eV

The band gap of a material is the energy difference between the highest occupied energy level (the valence band) and the lowest unoccupied energy level (the conduction band) in its electronic band structure. This energy gap determines the material's electrical conductivity and its ability to function as a semiconductor.

The band gaps of GaN-Ti (8,0), GaN-Ti (9,0), and GaN-Ti (10,0) single-walled nanotubes (SWNTs), with one Ti atom doped into the GaN structure, are 1.799 eV, 1.523 eV, and 1.437 eV respectively at gamma ($1 \times 1 \times 1$) k-points.

3.1.3 Effect of Titanium (Ti) Doping on the Band Structure and Band Gap of GaN

Doping Gallium Nitride (GaN) with Titanium (Ti) introduces significant changes to its electronic properties, specifically the band structure and band gap. Here's a breakdown of how Ti doping affects these characteristics:

1. Introduction of Impurity Levels

- When Ti atoms are introduced into the GaN lattice, they act as impurity atoms.
- Titanium has different electronic properties than Gallium (Ga) and Nitrogen (N), so its presence creates new impurity energy levels within the GaN band gap.
- These impurity levels can introduce donor (electron) or acceptor (hole) states, depending on the interaction between Ti and GaN, thus modifying the material's band structure.

2. Reduction of Band Gap

- Ti doping typically results in a reduction of the GaN band gap.
- The impurity levels introduced by Ti atoms lie within the existing GaN band gap, effectively decreasing the energy difference between the valence and conduction bands.
- This reduction makes GaN more conductive, especially under thermal or optical excitation, as electrons need less energy to transition from the valence band to the conduction band.

3. Enhanced Conductivity

- By reducing the band gap, Ti doping increases the electrical conductivity of GaN.
- The introduction of impurity levels close to the conduction or valence bands serves as pathways for electrons or holes, enhancing carrier mobility within the material.
- This improved conductivity makes Ti-doped GaN more suitable for applications that require higher conductivity, such as high-power electronic devices.

4. Possible Structural Distortions

- Doping can also induce distortions in the GaN lattice structure, as Ti atoms have different atomic sizes compared to Ga and N atoms.
- These structural distortions can further influence electronic properties by affecting the band structure, possibly creating localized states or shifting existing bands.

3.1.4 Density of States and Partial Density of States

The Density of States (DOS) and Partial Density of States (PDOS) are vital concepts in solid-state physics and materials science, crucial for understanding the electronic properties of materials.

The DOS quantifies the number of electronic states per unit energy available for occupation in a solid. It is mathematically expressed as:

$$g(E) = \frac{1}{(2\pi)^3} \int \delta(E - E(k)) d^3k$$

where $E(k)$ is the energy dependent on the wave vector k . A higher DOS indicates more available electronic states, influencing the material's electrical, thermal, and optical properties, and is particularly relevant in differentiating conductors, semiconductors, and insulators.

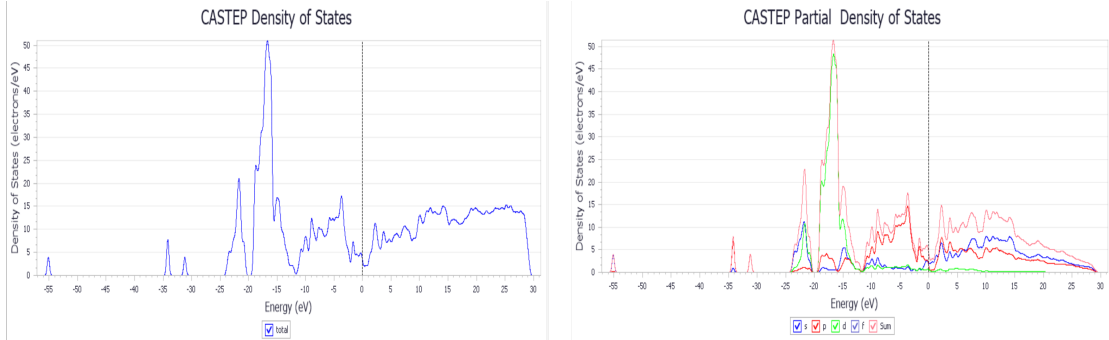
In contrast, the PDOS provides a breakdown of how specific atomic orbitals or sites contribute to the overall density of states. This concept is expressed as:

$$g_i(E) = \frac{1}{(2\pi)^3} \int \delta(E - E(k)) \cdot |\phi_i(k)|^2 d^3k$$

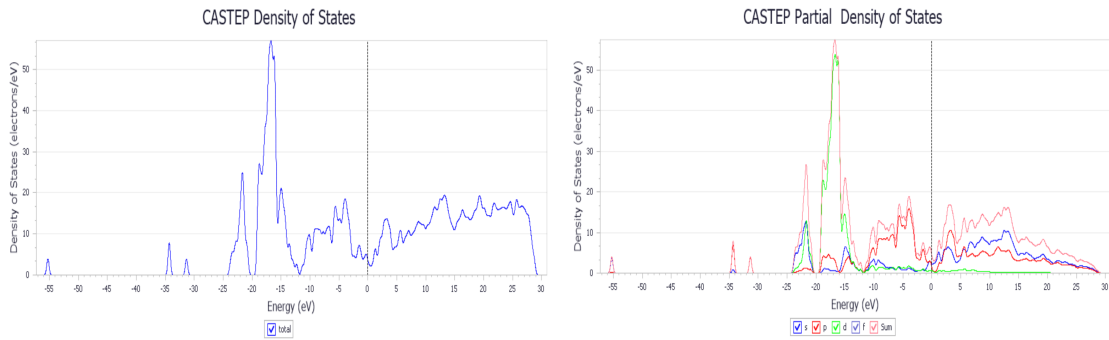
where $\phi_i(k)$ is the wave function of the i -th orbital. The PDOS helps identify the contributions of various orbitals to the electronic states at specific energy levels, which is especially useful in complex materials and nanostructures.

Together, DOS and PDOS are essential for characterizing the electronic behavior of materials.

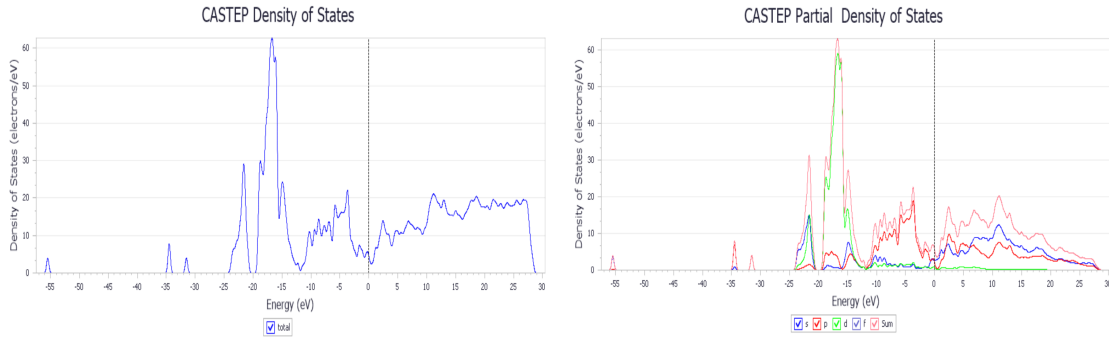
Doping has a significant impact on the Density of States (DOS) in materials, altering their electronic and optical properties. When a material is doped, the introduction of impurities such as donor or acceptor atoms shifts the Fermi level. For instance, n-type doping (where donor atoms are added) shifts the Fermi level closer to the conduction band, increasing the number of conduction electrons, while p-type doping (where acceptor atoms are added) moves the Fermi level closer to the valence band, increasing the number of holes. This shift in Fermi level changes the DOS near these energy states. Additionally, doping introduces impurity states within the material's band gap.



(a) DOS and PDOS for SWNT (8,0).

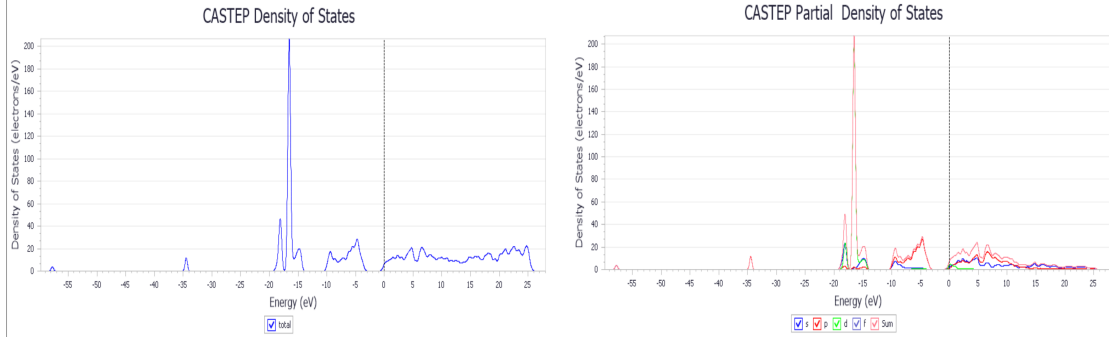


(b) DOS and PDOS SWNT (9,0).



(c) DOS and PDOS for SWNT (10,0).

Figure 16: Density of states and partial density of states plot of one Titanium atom doped at $3 \times 3 \times 6$ k-points (a) GaN (8,0) (b) GaN (9,0) (c) GaN (10,0)



(a) DOS and PDOS crystal Bulk

Figure 17: Density of states and partial density of states plot of one Titanium atom doped at $3 \times 3 \times 6$ k-points (a) GaN (8,0) (b) GaN (9,0) (c) GaN (10,0)

Table 4: GaN Nanotube Doping Information

GaN Nanotube	No. of atoms in Doped GaN						Band gap (eV) Ti doped at Ga-site	
	When doped at Ga-site			When doped at N-site				
	Ga	Ti	N	Ga	Ti	N		
GaN (10,0)	19	1	20	20	1	19	1.437	
GaN (9,0)	17	1	18	18	1	17	1.523	
GaN (8,0)	15	1	16	16	1	15	1.799	

Effect on Band Gap Ti doping typically reduces the band gap of GaN. This is because Ti introduces impurity states into the material, which can narrow the energy gap between the valence and conduction bands. As a result, the material may transition from being a wide-band-gap semiconductor to one with a more moderate gap,

Effect on Conductivity Doping with Ti increases the electrical conductivity of GaN. This occurs due to the introduction of impurity levels that provide additional free carriers (electrons or holes), which enhances charge transport in the material.

Band Structure Modification Ti doping modifies the band structure by adding impurity levels, which can cause band shifts. These impurity levels can act as electron donors or acceptors, depending on the doping concentration and the type of material. These changes influence both the optical and electronic properties of GaN,

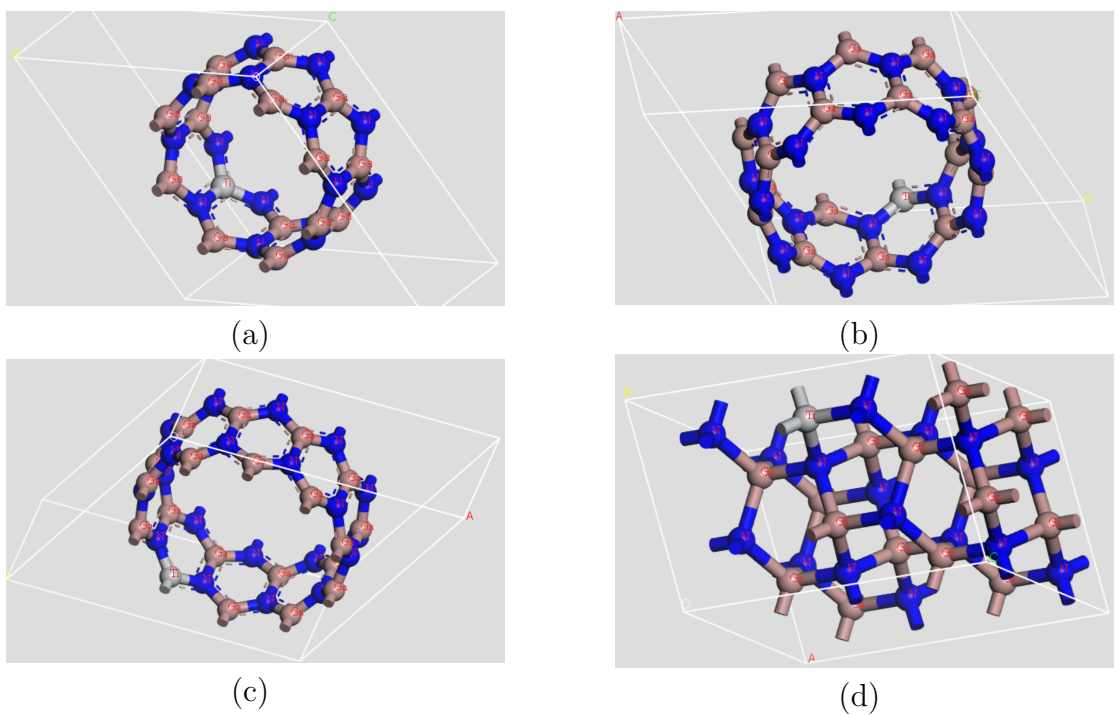


Figure 18: one Titanium atom doped with GaN (a) GaN-Ti (8,0), (b) GaN-Ti (9,0), (c) GaN-Ti (10,0), and (d) GaN-Ti crystal.

3.2 Calculation and analysis using Forcite tool

Forcite is a powerful module within the Materials Studio software suite, developed by BIOVIA (formerly Accelrys). It enables users to perform classical molecular dynamics (MD) simulations and energy minimizations using various forcefields, making it especially valuable for studying the properties and behavior of materials at the atomic and molecular levels. One of its key features is the ability to simulate atomic motion under realistic conditions, allowing researchers to analyze dynamic processes such as diffusion, thermal properties, and phase transitions. Energy minimization is another crucial function, where Forcite helps find the system's lowest energy configuration by optimizing atomic positions. The module supports a variety of forcefields like COMPASS, Dreiding, and Universal, making it versatile for simulating different material types, including metals, polymers, ceramics, and nanomaterials. Forcite also calculates thermodynamic properties such as heat capacity, entropy, and free energy, providing essential insights into a material's stability and performance. Furthermore, it facilitates structural optimization of bulk materials, surfaces, interfaces, and even nanostructures like nanotubes, which is particularly useful in advanced materials research. Additionally, Forcite can simulate mechanical deformation and analyze stress-strain behavior, helping to understand the mechanical properties of materials. It finds wide application in studying nanomaterials, polymers, and bulk materials, providing insights into their structural stability, mechanical behavior, and phase transitions.

Use Cases:

- Nanomaterials: Forcite is widely used to simulate the behavior of nanomaterials, such as nanotubes or nanoparticles, by providing insights into structural stability and mechanical properties under various conditions.
- Polymers: It is particularly useful for modeling polymeric materials and their interactions, helping in the design of new materials with desirable mechanical and thermal properties.
- Crystals and Bulk Materials: Researchers use Forcite to study defects, grain boundaries, and phase transitions in bulk materials.

First-principles calculations play a critical role in understanding the phonon properties of materials, providing insights into their thermal, elastic, and dynamic behaviors. These calculations, based on density functional theory (DFT), allow scientists to predict how atoms vibrate in a solid and how these vibrations affect a material's properties.

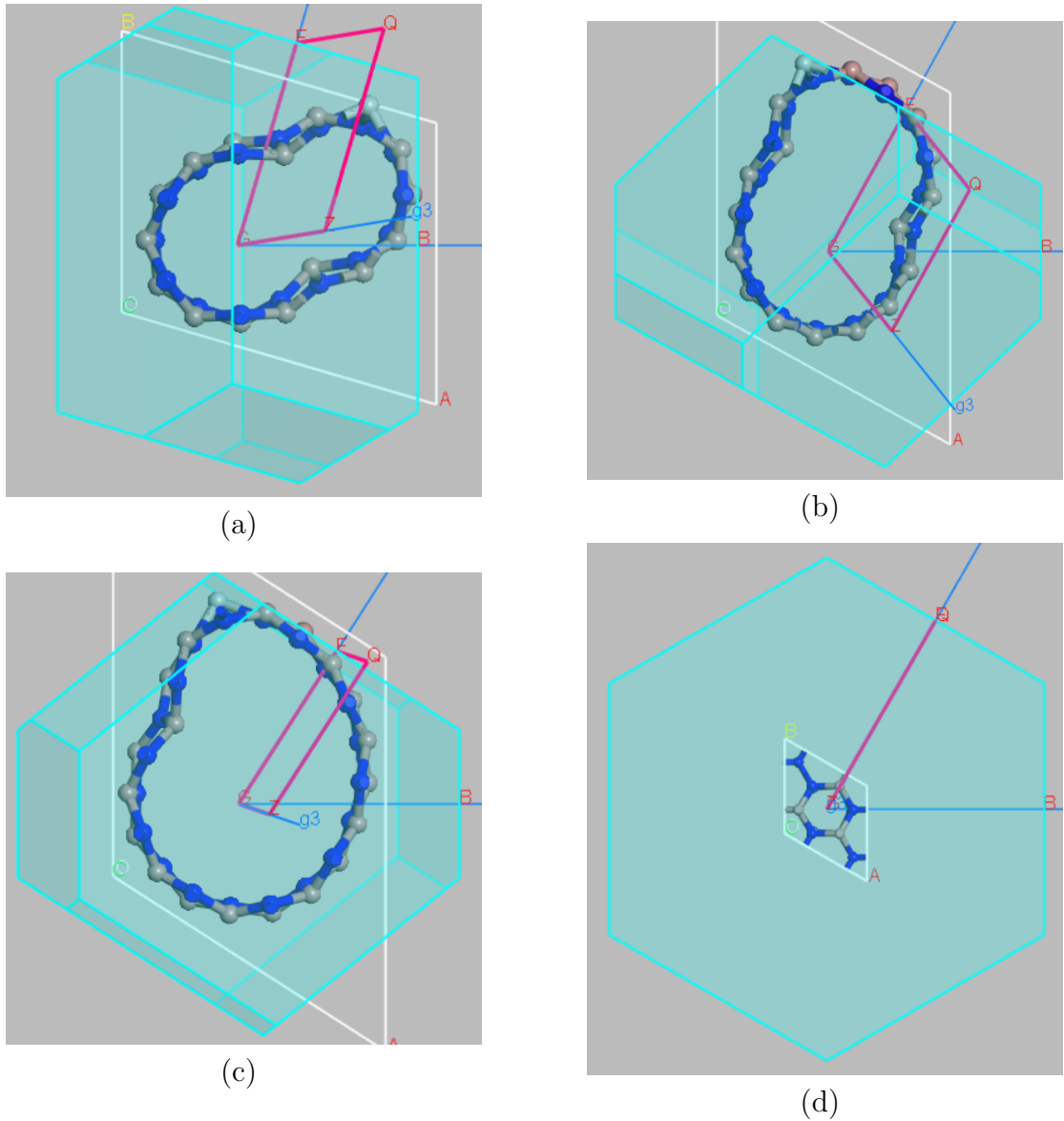


Figure 19: Brillouin Zone Structure obtained through Geometry optimization GaN with Ti doped: (a) GaN-Ti (8,0), (b) GaN-Ti (9,0), (c) GaN-Ti (10,0), and (d) GaN-Ti crystal.

3.3 Mechanical properties

The Forcite module in Materials Studio allows users to calculate various mechanical properties using molecular dynamics (MD) simulations. It can perform energy calculations, geometry optimizations, and evaluate mechanical properties like stress-strain relationships by running simulations based on atomic models of materials.

To calculate mechanical properties such as stress-strain diagrams, Forcite can be used with a proper setup of forcefields, input configurations, and simulation parameters. Users can input materials' models (such as nanocomposites or alloys) and run simulations to derive key mechanical properties like elasticity, tensile strength, and modulus.

We have used ELATE (Elastic Tensor Analysis) which is an open-source tool designed for analyzing and visualizing the elastic properties of materials. It can process the elastic tensor of materials and provide a detailed analysis of mechanical properties, including anisotropy, Young's modulus, shear modulus, and Poisson's ratio. ELATE is particularly useful for materials with anisotropic behavior and can visualize these properties in various orientations.

Elastic analysis of materials involves understanding how a material deforms under stress and returns to its original shape when the stress is removed. This analysis is essential in studying the mechanical properties of materials, such as Young's modulus, shear modulus, and Poisson's ratio. These properties help predict how materials will perform under various forces and conditions.

The Voigt, Reuss, and Hill schemes are methods used to average material properties and predict how a material will respond under mechanical stress. The Voigt method assumes uniform strain throughout the material, while the Reuss method assumes uniform stress. The Hill method offers a compromise by averaging the results from both Voigt and Reuss. Key material properties include the bulk modulus, which measures the material's resistance to uniform compression—higher values indicate less compressibility. Young's modulus describes the material's stiffness, reflecting how much it will deform under tension or compression. The shear modulus, on the other hand, represents the material's ability to resist shear stress, such as when forces are applied in opposite directions parallel to the surface. Poisson's ratio gives insight into how much a material contracts in directions perpendicular to an applied force. Finally, the eigenvalues of the stiffness matrix characterize how the material responds to stress in different directions, showing how easily it deforms under complex loading conditions. Together, these properties provide a comprehensive view of a material's elastic behavior under stress.

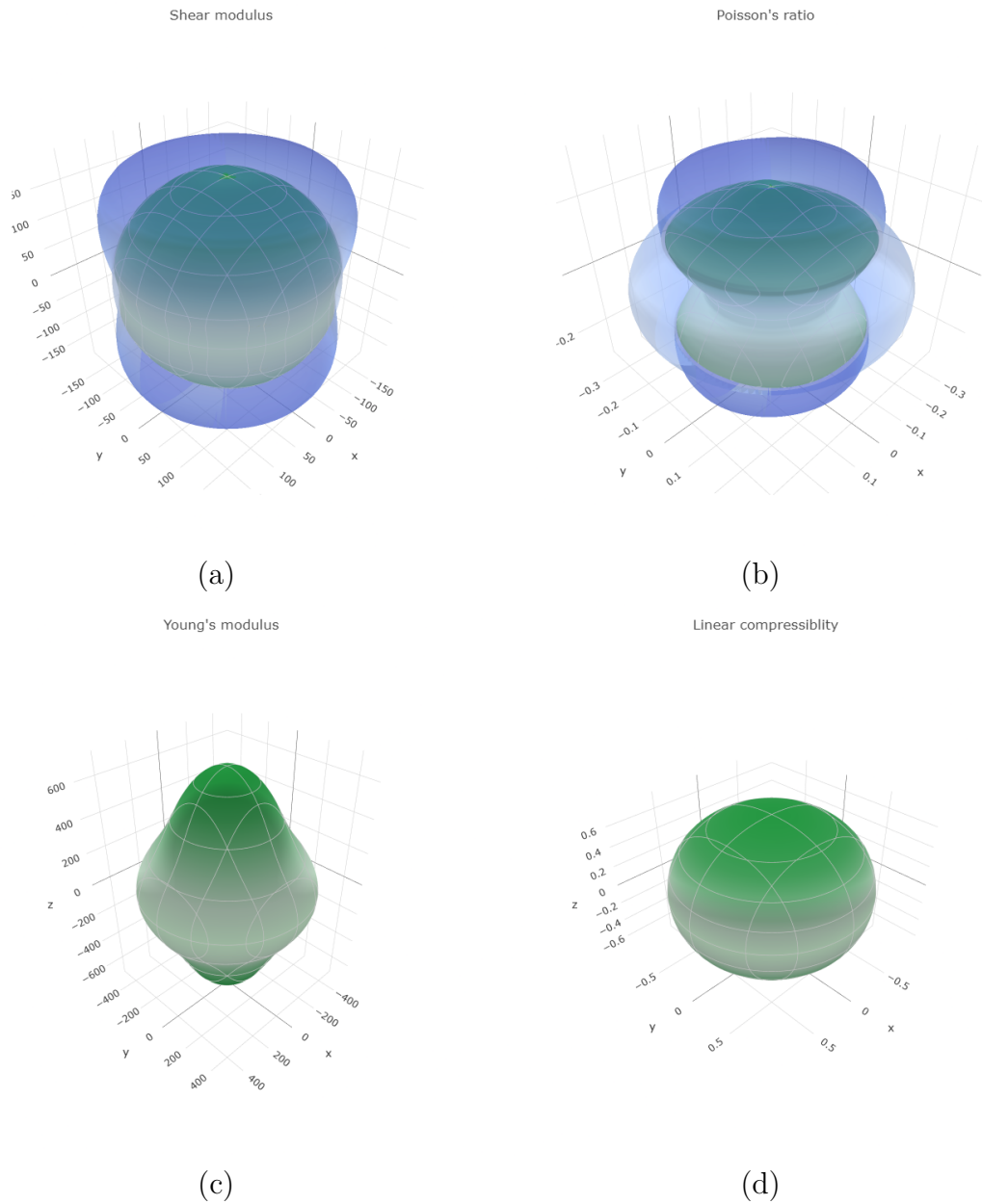
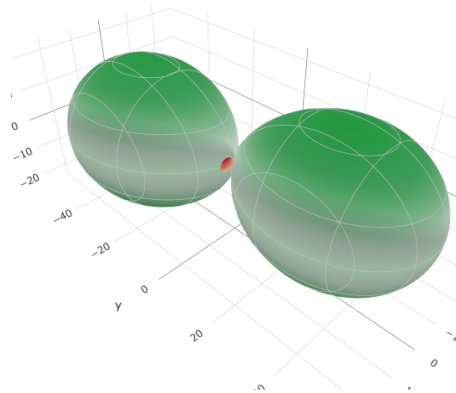


Figure 20: Mechanical properties of Geometry optimized GaN-Ti bulk crystal: (a) Shear modulus, (b) Poissons ratio, (c) Youngs modulus, and (d) Linear compressibility.

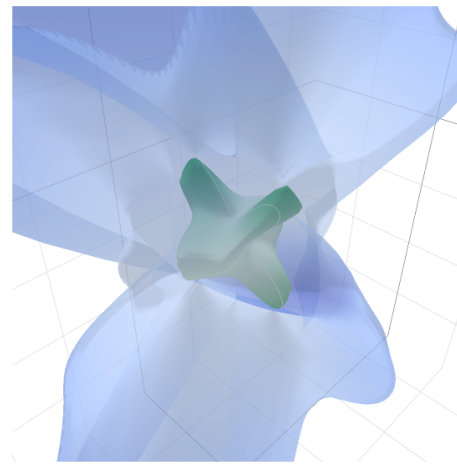
Linear compressibility

Shear modulus



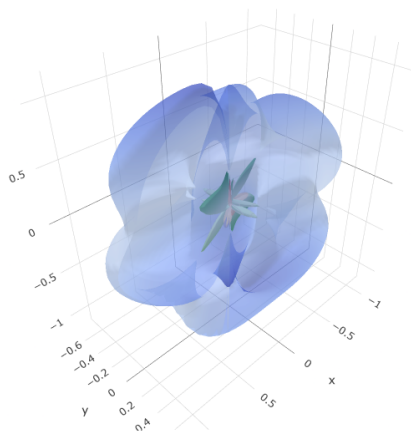
(a)

Poisson's ratio

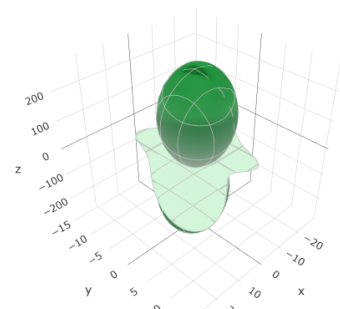


(b)

Young's modulus



(c)



(d)

Figure 21: Mechanical properties of Geometry optimized GaN-Ti SWNT (8,0): (a) Linear compressibility, (b) Shear modulus, (c) Poissons ratio, and (d) Youngs modulus.

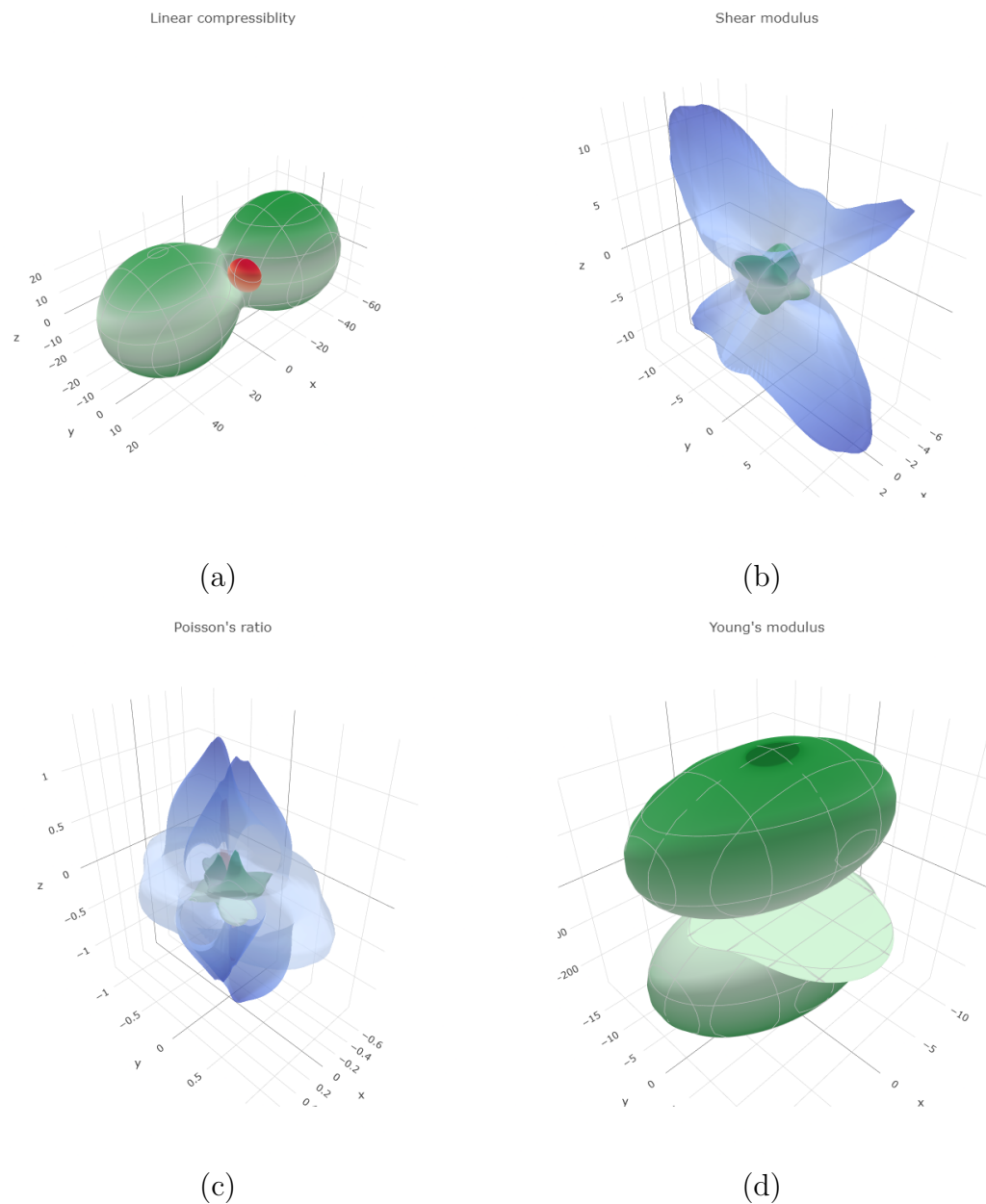
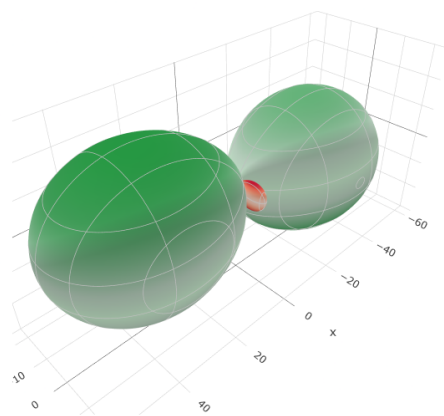


Figure 22: Mechanical properties of Geometry optimized GaN-Ti SWNT (9,0): (a) Linear compressibility, (b) Shear modulus, (c) Poissons ratio, and (d) Youngs modulus.

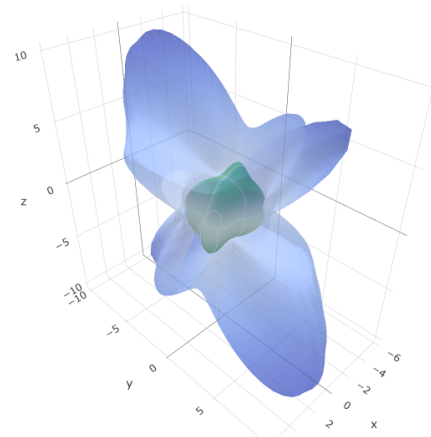
Linear compressibility



(a)

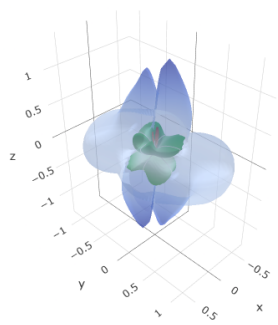
Poisson's ratio

Shear modulus

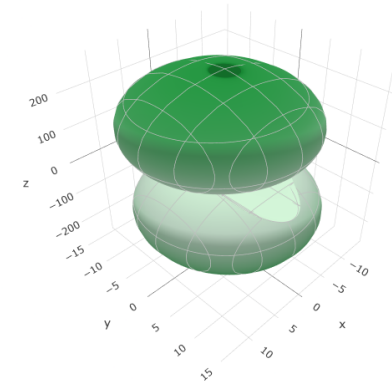


(b)

Young's modulus



(c)



(d)

Figure 23: Mechanical properties of Geometry optimized GaN-Ti SWNT (10,0):
 (a) Linear compressibility, (b) Shear modulus, (c) Poissons ratio, and (d) Youngs modulus.

Table 5: Mechanical properties Bulk and SWNT structures

Structures	Bulk	SWNT (8,0)	SWNT (9,0)	SWNT (10,0)
Total potential energy	-43.23851844	-16.80410156	-14.45658964	-2.01356162
Bond energy	8.50775669	0.79058043	0.76197666	0.52309612
Angle energy	58.45907902	20.77346464	23.08422790	30.79047302
Torsion energy	30.30288166	43.50779723	46.35813679	45.89579087
Inversion energy	N/A	1.82305391	4.93751295	13.77992701
van der Waals energy	-138.41134731	-82.51168985	88.31765386	91.67555016
Total valence energy	97.26971737	66.89489622	75.14185431	90.98928702
Non-bond energy	-140.50823581	-83.69899778	-89.59844395	-93.0028464
Density	6.32180372	3.57955499	3.41577521	3.17356118
Cell volume	346.20711691	611.43171264	722.16911402	864.92149389
Length a	6.22192673	12.03863467	11.11695381	12.51566250
Length b	6.22192661	10.09535131	14.53996404	15.19481488
Length c	10.32655789	5.35976798	5.38125285	5.42068865
Angle alpha	90.00000007	92.17012515	77.97513366	88.58325233
Angle beta	89.99999964	101.87473020	104.15590978	94.23102382
Angle gamma	120.00000028	105.45459906	120.61565066	122.70632991

4 Conclusion

In conclusion, The study of structural, electronic, and elastic properties plays a crucial role in understanding the behavior of materials like GaN-Ti, both in bulk and nanotube forms. Titanium (Ti) doping in Gallium Nitride (GaN) significantly alters the material's characteristics. Structurally, Ti introduces changes in the atomic arrangement and bond lengths, enhancing the material's stability and modifying its lattice parameters. This, in turn, influences the material's mechanical properties, making it more adaptable for high-performance applications. Electronically, Ti doping reduces the band gap of GaN, which can improve charge transport and enhance the material's conductivity. These modifications in the electronic structure are vital for optoelectronic devices, including light-emitting diodes (LEDs) and other semiconductor applications. Additionally, the elastic properties of GaN-Ti nanotubes show enhanced mechanical strength and flexibility when compared to pure GaN, which makes it suitable for applications that require materials with high mechanical integrity and resilience. The combined effects of these changes suggest that Ti-doped GaN materials offer a promising pathway for advanced technological applications in electronics, energy, and nanotechnology.

5 References

Academic Papers and Books

- Baroni, S., de Gironcoli, S., Dal Corso, A., & Giannozzi, P. (2001). Phonons and related crystal properties from density-functional perturbation theory. *Reviews of Modern Physics*, 73(2), 515.
- Gonze, X., & Lee, C. (1997). Dynamical matrices, Born effective charges, dielectric permittivity tensors, and interatomic force constants from density-functional perturbation theory. *Physical Review B*, 55(16), 10355.
- Zhang, Z., & Sun, X. (2011). First-principles study of the electronic and structural properties of GaN nanotubes. *Journal of Applied Physics*, 110(8), 083713.
- Seifert, G., Hernández, E., & Terrones, H. (2000). On the electronic structure of GaN nanotubes. *Physical Review B*, 62(22), 15819.
- Togo, A., Oba, F., & Tanaka, I. (2008). First-principles calculations of the ferroelastic transition between rutile-type and CaCl₂-type SiO₂ at high pressures. *Physical Review B*, 78(13), 134106.
- Alfe, D. (2009). PHON: A program to calculate phonons using the small displacement method. *Computer Physics Communications*, 180(12), 2622-2633.
- Clark, S. J., Segall, M. D., Pickard, C. J., Hasnip, P. J., Probert, M. I., Refson, K., & Payne, M. C. (2005). First principles methods using CASTEP. *Zeitschrift für Kristallographie-Crystalline Materials*, 220(5-6), 567-570.
- Accelrys Inc. (2020). Forcite User Guide. Accelrys Software Inc.
- Peelaers, H., Kioupakis, E., & Van de Walle, C. G. (2014). Free-carrier absorption in transparent conducting oxides: Phonon and impurity scattering mechanisms. *Physical Review B*, 92(23), 235201.
- Broido, D. A., Malorny, M., Birner, G., Mingo, N., & Stewart, D. A. (2007). Intrinsic lattice thermal conductivity of semiconductors from first principles. *Applied Physics Letters*, 91(23), 231922.
- Mingo, N., & Broido, D. A. (2005). Carbon nanotube ballistic thermal conductance and its limits. *Physical Review Letters*, 95(9), 096105.
- Radovanović, M., Stamenković, D., Milošević, I., & Šušteršić, L. (2015). Ab initio study of phonons in GaN nanowires. *Journal of Physics D: Applied Physics*, 48(38), 385304.
- Wang, Q., Zhang, H., & Liu, Z. (2013). Structural and electronic properties of GaN nanotubes under uniaxial strain: A first-principles study. *Computational Materials Science*, 67, 256-261.

- Lee, K., Murray, É. D., Kong, L., Lundqvist, B. I., & Langreth, D. C. (2010). Higher-accuracy van der Waals density functional. *Physical Review B*, 82(8), 081101.
- Giannozzi, P., Baroni, S., Bonini, N., Calandra, M., Car, R., Cavazzoni, C., & Dal Corso, A. (2009). QUANTUM ESPRESSO: a modular and open-source software project for quantum simulations of materials. *Journal of Physics: Condensed Matter*, 21(39), 395502.
- Fultz, B. (2010). Vibrational thermodynamics of materials. *Progress in Materials Science*, 55(4), 247-352.
- Wang, H., Shi, X., & Chen, L. (2007). Thermoelectric properties of metal-doped GaN nanotubes: A first-principles study. *Journal of Applied Physics*, 101(4), 043701.
- Payne, M. C., Teter, M. P., Allan, D. C., Arias, T. A., & Joannopoulos, J. D. (1992). Iterative minimization techniques for ab initio total-energy calculations: molecular dynamics and conjugate gradients. *Reviews of Modern Physics*, 64(4), 1045.
- Gale, J. D., & Rohl, A. L. (2003). The General Utility Lattice Program (GULP). *Molecular Simulation*, 29(5), 291-341.
- Terrones, M., Terrones, H., Hernández, E., Grobert, N., Charlier, J. C., & Ajayan, P. M. (2000). New direction in nanotube science. *Nature*, 388(6643), 52-59.
- Lawler, H. M., & Hart, G. L. W. (2007). Phonons and electronic structure of small-diameter nanotubes. *Physical Review B*, 76(4), 045117.
- Yan, Q., Rinke, P., Janotti, A., & Van de Walle, C. G. (2012). First-principles study of the electronic properties of TiN. *Applied Physics Letters*, 101(7), 072105.
- Mastro, M. A., Bertness, K. A., & Teichert, J. A. (2010). *Gallium Nitride: Materials and Devices*. CRC Press.